Magnetoresistance Due to Chaos and Nonlinear Resonances in Lateral Surface Superlattices

R. Fleischmann, T. Geisel, and R. Ketzmerick

Institut für Theoretische Physik und Sonderforschungsbereich Nichtlineare Dynamik, Universität Frankfurt, D-6000 Frankfurt/Main 11, Federal Republic of Germany

(Received 3 December 1991)

We show that chaos and nonlinear resonances are clearly reflected in the magnetotransport in lateral surface superlattices and thereby explain a series of magnetoresistance peaks observed recently in "antidot" arrays on semiconductor heterojunctions. We find a mechanism of cyclotron-orbit pinning in an electric field resulting from Kolmogorov-Arnol'd-Moser tori. An experimental verification is suggested in terms of an enhanced cyclotron frequency associated with an anomalously reduced cyclotron radius.

PACS numbers: 73.40.Kp, 05.45.+b, 73.50.Jt

In the last few years many laboratories have achieved the preparation of periodic submicron structures in semiconductor heterojunctions known as lateral surface superlattices (LSSLs) [1]. Several kinds of LSSLs are used in experiments, e.g., one- and two-dimensional (2D) weak and strong modulation of the 2D electron gas (2DEG), arrays of quantum dots, i.e., 2D potential wells, and "antidots," i.e., reflecting potential peaks. Magnetoresistance, Hall effect, and far-infrared measurements show many peculiarities [2–6]. The long-standing goal of observing Hofstadter's self-similar energy spectrum [7] in these samples is still not accomplished; it might be inachievable as classical chaos can modify the Hofstadter butterfly considerably [8]. In the currently investigated samples the superlattice spacing is larger than the Fermi wavelength and thus the dynamics of a wave packet approaches the classical limit. Classical nonchaotic [9] and chaotic [10,11] electron dynamics has been investigated in different models of LSSLs. Experimental support stems, e.g., from recent magnetoresistance measurements in 2D antidot arrays [5,6], where a series of peaks in $R_{xx}(B)$ not present in the unmodulated 2DEG was found [see, e.g., the dotted line in Fig. 3(e)] and explained using a billiard model of reflecting disks and an *ad hoc* assumption of pinned classical cyclotron orbits [5]. Circular orbits enclosing 1, 2, 4, 9, or 21 antidots without colliding [similar to those in Fig. 1(a)] were assumed not to respond to an electric field. This assumption is justified by its success, but is not fulfilled within the billiard model itself. Thus an important question is what could be the physical nature of such a pinning mechanism. Another serious problem is an observed extra peak [5], which becomes predominant in samples of smaller electron densities [see, e.g., peak X in Fig. 3(f)]. It belongs to a magnetic field that cannot be associated with a collision-free cyclotron orbit and it thus cannot be explained within this scheme.

In the present Letter we investigate magnetotransport in a model assuming a *continuous* antidot potential and find that chaos and Kolmogorov-Arnol'd-Moser (KAM) theory are reflected in the observed magnetoresistance peaks. We demonstrate the existence of a pinning mechanism and explain its nature by islands of regular motion due to nonlinear resonances. We then formulate a theoretical framework for frequency-dependent conductivities in LSSLs, which includes regular and chaotic motion as well as random elastic scattering at impurities. It reproduces the observed magnetoresistance peaks without adjustable parameters, where surprisingly the pinned orbits themselves play only a minor role. We show that the peaks are caused mainly by the correlation function of unperturbed chaotic motion, which also reflects the presence of nonlinear resonances. The observed extra peak is explained by a particular nonlinear resonance in the continuous potential. It has an anomalously reduced cyclotron radius and we consequently predict an augmented cyclotron frequency to show up in far-infrared experiments. These results confirm that transport experiments in modulated 2DEGs can be explained in terms of classical nonlinear dynamics.

The classical approximation for the dynamics of an

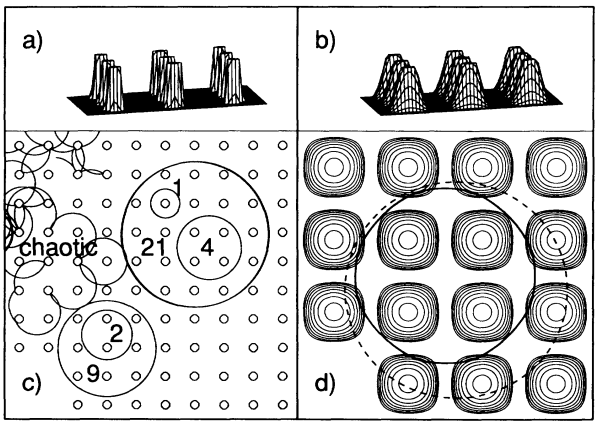

FIG. 1. (a),(b) The 2D antidot potential [Eq. (3)] for $\beta=64$ (steep potential) and $\beta=4$ (smooth potential). (c) Regular orbits for different magnetic fields in the steep potential surrounding 1, 2, 4, 9, and 21 antidots and a chaotic orbit. (d) Regular orbit for $B/B_0\approx 0.3$ (solid line) deflected by the smooth potential (visualized by equipotential lines) such that its radius is smaller than that of a free cyclotron orbit (dashed line).

electron wave packet in a 2D potential $U(x,y)$ and a perpendicular magnetic field $\mathbf{B}$ is described by the Hamiltonian

$$H=(\mathbf{p}-e\mathbf{A})^2/2m+U(x,y)\,, \tag{1}$$

where $\mathbf{A}$ is the vector potential and m the effective mass of the electron. We introduce dimensionless variables $\tilde{x}=x/a$, $\tilde{y}=y/a$, $\tilde{t}=t/\tau_0$, $\tilde{H}=H/\epsilon_F$, $\tilde{U}=U/\epsilon_F$, where a is the lattice constant of the artificial structure, ϵ_F the Fermi energy, and $\tau_0=(\epsilon_F/ma^2)^{1/2}$, and we scale the magnetic field by $B_0=2(2m\epsilon_F)^{1/2}/ea$, where $B=B_0$ corresponds to a free cyclotron radius of $a/2$. Choosing the gauge $\mathbf{A}=-\mathbf{r}\times\mathbf{B}/2$ for the vector potential and omitting the tildes, the equations of motion read

$$\begin{aligned}&\dot{x}=v_x,\quad \dot{v}_x=2\sqrt{2}(B/B_0)v_y-\partial U/\partial x\,,\\ &\dot{y}=v_y,\quad \dot{v}_y=-2\sqrt{2}(B/B_0)v_x-\partial U/\partial y\,.\end{aligned} \tag{2}$$

To model antidot arrays we will use the potential

$$U(x,y)=U_0[\cos(2\pi x)\cos(2\pi y)]^{\beta}\,, \tag{3}$$

where β controls the steepness of the antidots. We consider a steep potential [$\beta=64$, Fig. 1(a)] and a smooth potential [$\beta=4$, Fig. 1(b)] resembling two distinct experimental situations. The prefactor U_0 of the potential is chosen such that the ratio of the dot diameter at the Fermi energy to the distance of adjacent dots is one-third, similar to the experiments [5].

Studying first the dynamics in the *absence* of an electric field we find orbits enclosing 1, 2, 4, 9, 21, and even more antidots for the steep potential, as well as chaotic orbits, as shown in Fig. 1(c). For the smooth potential we find orbits enclosing 1 and 4 antidots, occurring with decreasing magnetic fields. This is similar to the hard-wall billiard model [5] where the potential is constant in the space between dots. With the analytic potential of Eq. (3), however, we are also able to understand the nature of the pinning mechanism. For this purpose we investigate the motion in *phase* space (x,y,v_x,v_y) by means of Poincaré surfaces of section (y,v_y) at $x(\mathrm{mod}1)=x_0$. A typical section [Fig. 2(a)] exhibits a sea of chaotic motion and an island of regular motion with an elliptic fixed point at its center ($y\approx 0.5$). This point represents an intersection with a cyclotron-type orbit of radius $\approx\frac{1}{2}$ revolving around a single antidot at $(x,y)=(0,0)$. Other unperturbed cyclotron orbits [i.e., for different initial conditions (y,v_y)] have turned into a motion on invariant tori (KAM tori [11,12]), whose intersections give the closed loops in the island. Generally such islands are known to result from nonlinear resonances between the degrees of freedom [12]. As B is decreased we find a series of resonances belonging to cyclotronlike orbits that enclose 1, 2, 4, 9, and 21 antidots. In an electric field in a hard-wall billiard model, cyclotron orbits would drift until they hit a wall and thus become a chaotic (unpinned) orbit. The effect of an applied electric field (along x) in the smooth potential is illustrated in Figs. 2(b) and 2(c), where an ensemble of orbits is generated by 5000 random initial conditions in a rectangular subregion at $x=0$ [Fig. 2(b)]. In Fig. 2(c) we plot only those orbits that return to the plane $x=0$ within a time interval $[t,t+\Delta t]$ at a later time $t\gg\Delta t$, where Δt is about twice the cyclotron period. Orbits started in the chaotic sea have escaped, whereas orbits in the regular island do not drift away, in spite of the applied electric field. This is plausible from, but not directly implied by, the KAM theorem [12]. Thus the pinning mechanism assumed in Ref. [5] is substantiated by the occurrence of regular islands due to nonlinear resonances. If a sufficiently strong electric field is applied, they can be destroyed of course.

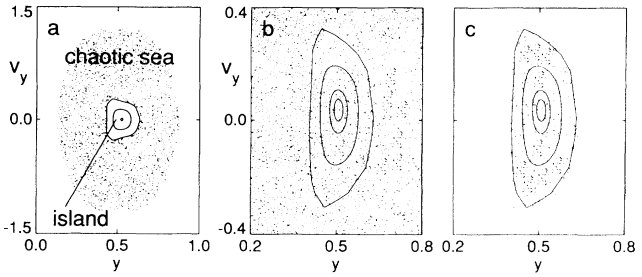

FIG. 2. (a) Poincaré surface of section [at $x(\mathrm{mod}1)=0$] for $B/B_0=1$ in the smooth potential, generated from four different initial conditions. The island of regular motion represents intersections of invariant tori for cyclotronlike orbits (radius $\approx\frac{1}{2}$) revolving around an antidot at $(x,y)=(0,0)$. (b) Randomly chosen *initial conditions* y and v_y for 5000 orbits started in a rectangular subregion covering the island and part of the chaotic sea with $x=0$ for $B/B_0=1$, and $\beta=4$. Lines indicate the intersection of invariant tori. (c) Intersection points of those orbits that in an applied electric field return to this region and thus remain "pinned."

A quantitative theory of the magnetoresistance moreover requires a detailed consideration of regular and chaotic orbits in the presence of impurity scattering. In conservative systems with two degrees of freedom the accessible phase space is the 3D energy surface Γ separated into disjunct parts Γ_i by invariant tori. For a microcanonical ensemble the conductivity tensor $\boldsymbol{\sigma}$ then is the sum of the individual conductivities $\boldsymbol{\sigma}^i$, weighted by their relative volume in phase space $p_i=V_i/V$,

$$\boldsymbol{\sigma}=\sum_i p_i\boldsymbol{\sigma}^i\,. \tag{4}$$

The pinned orbits do not respond to a weak electric field ($\boldsymbol{\sigma}^p\equiv 0$) and the conductivity is due to chaotic orbits only,

$$\boldsymbol{\sigma}=p_c\boldsymbol{\sigma}^c=(1-p_p)\boldsymbol{\sigma}^c\,. \tag{5}$$

Variation of the magnetic field changes the portion p_p of pinned orbits as well as the conductivity $\boldsymbol{\sigma}^c$ of the chaotic orbits. In previous work Weiss *et al.* [5] determined p_p in the billiard model, but assumed σ^c to be the Drude conductivity with an increased scattering rate due to the

reflecting disks. It will become clear later that it is essential to consider the chaotic dynamics in detail to determine σ^c. Lorke, Kotthaus, and Ploog [6] determined the total σ from the Einstein relation, which neglects the pinning of regular orbits.

At low temperatures elastic impurity scattering needs to be considered. Thereby a pinned orbit may become a chaotic orbit and vice versa, but the ratio of pinned to chaotic orbits is not changed and their contributions can still be summed up as in Eq. (4). In order to incorporate impurity scattering into the calculation of σ^c we use classical linear response theory [13] for the frequency-dependent conductivity,

$$\sigma_{ij}(\omega)=\frac{ne^2}{k_BT}\int_0^\infty dt\, C_{ij}(t)e^{i\omega t}, \tag{6}$$

where $C_{ij}(t)=\langle v_i(t)v_j(0)\rangle_\Gamma$ is the velocity correlation function averaged over phase space, n is the 2D electron density, k_B the Boltzmann constant, and T the temperature. Assuming statistical independence of the scattering events the probability that there is no scattering in the time interval $[0,t]$ is $P(t)=\exp(-t/\tau)$, where τ is the average time between two impurity scatterings. Dividing the correlation function into a contribution from unperturbed orbits, i.e., which do not undergo scattering up to time t (marked by a tilde), and a contribution from orbits that scatter at least once (marked by a caret), we find

$$\begin{aligned}C_{ij}(t)&=P(t)\tilde{C}_{ij}(t)+[1-P(t)]\hat{C}_{ij}(t)\\&=\exp(-t/\tau)\tilde{C}_{ij}(t),\end{aligned} \tag{7}$$

where we have used $\hat{C}_{ij}(t)=0$ [14] as impurity scattering destroys any correlations. According to Eq. (7) the correlation function factorizes into an exponential decay due to impurity scattering and the unperturbed deterministic correlation function. From Eqs. (4)–(7) we finally obtain the conductivity as

$$\begin{aligned}\sigma_{ij}(\omega,\tau)&=(1-p_p)\sigma_{ij}^c(\omega,\tau)\\&=(1-p_p)\frac{ne^2}{k_BT}\int_0^\infty dt\, e^{(-1/\tau+i\omega)t}\langle\tilde{v}_i(t)\tilde{v}_j(0)\rangle_{\Gamma_c},\end{aligned} \tag{8}$$

where the correlation function solely includes unperturbed chaotic orbits and is easy to obtain numerically.

For a numerical computation of σ_{ij} as a function of B we first determine the portion p_p of pinned electrons using Poincaré surfaces of section [15]. For the steep potential it exhibits peaks corresponding to maxima of the volume of regular regions for orbits enclosing 1, 2, 4, and 9 antidots [Fig. 3(a)]. In the smooth potential there are peaks for orbits enclosing 1 and 4 antidots [Fig. 3(b)]. Next we compute $\tilde{C}_{ij}(t)=\langle\tilde{v}_i(t)\tilde{v}_j(0)\rangle_{\Gamma_c}$ by numerical integration of Eq. (2). Choosing a typical experimental value for the mean scattering time $\tau\approx 4\times10^{-11}$ s we obtain the contribution to the conductivity σ^c and magnetoresistance $R_{xx}^c=\sigma_{xx}^c/(\sigma_{xx}^{c2}+\sigma_{xy}^{c2})$ that is due to the correlation functions of chaotic orbits. We emphasize that these results [Figs. 3(c) and 3(d)] clearly deviate from a Drude ansatz [5], which would yield a magnetoresistance $R_{xx}^c=m/n\tau_{\rm eff}e^2$ constant in B. R_{xx}^c already anticipates all details of the total magnetoresistance R_{xx} according to Eq. (8) shown in Figs. 3(e) and 3(f). Surprisingly the magnetoresistance peaks mainly are not caused by the varying number p_p of pinned (regular) orbits [Figs. 3(a) and 3(b)], but by correlations within the chaotic sea, which also show structure reflecting the presence of nonlinear resonances. This is because chaotic orbits in the vicinity of regular islands tend to follow their dynamics for a long time [10,11]. These numerical results are in good agreement with experiments by Weiss *et al.* [5] [dotted lines in Figs. 3(e) and 3(f)], who varied the electron density in their samples using the persistent photoconductivity effect, and thereby varied the steepness of the antidot potential.

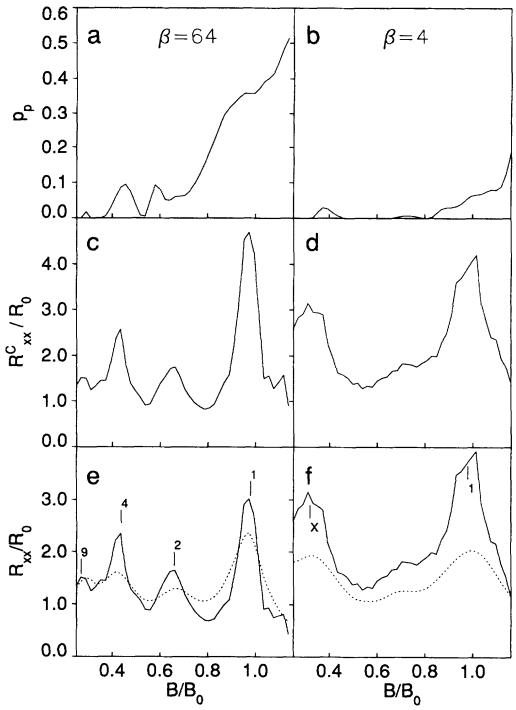

FIG. 3. Magnetic field dependence (a),(b) of the portion p_p of pinned orbits, (c),(d) of the magnetoresistance R_{xx}^c associated with chaotic correlations, and (e),(f) of the total magnetoresistance normalized to the zero-field resistance R_0, in the steep (left) and the smooth (right) potentials. The peaks in (e) and (f) are marked by the number of antidots that are enclosed within respective cyclotronlike regular orbits, and (without adjustable parameters) agree well with experiments (dotted lines) by Weiss *et al.* (samples 3* and 1* of Ref. [5]).

Note that the theory has no adjustable parameters, since the R scale can be normalized to the zero-field resistance R_0 and $B_0=(8\pi\hbar^2n)^{1/2}/ea$ is determined by the experimental values of a, m, and n. The values of the dot diameter and the parameters τ and β are not known with

sufficient accuracy. If these were considered adjustable parameters, the agreement would probably improve.

In the steep potential, corresponding to a sample of high electron density, peaks occur at magnetic fields where cyclotronlike orbits enclosing 1, 2, 4, and 9 antidots show up. For the smooth potential, which models a sample of lower electron density, we find peaks associated with orbits enclosing 1 and 4 antidots. The latter is shifted to a notably lower magnetic field (peak X), where in a billiard model a collision-free cyclotron orbit cannot exist [see, e.g., Fig. 1(d)]. It thus explains the predominant extra peak that was found to be inconsistent with a simple billiard model [5]. Here the peak is explained by an anomalously reduced cyclotron radius due to deflections from the smooth superlattice potential [see Fig. 1(d)]. This is possible only by a nonlinear resonance and underlines the importance of nonlinear dynamics in a continuous potential. As a consequence of the reduced radius we predict an augmented cyclotron frequency to show up in far-infrared spectroscopy [16]. Finally, also the observed shoulder near $B/B_0 \approx 0.7$ is reproduced. It has a similar origin and belongs to another cyclotronlike orbit with an anomalously reduced radius enclosing a single antidot. These results will be presented in more detail elsewhere.

We acknowledge helpful discussions with D. Weiss, M. L. Roukes, A. Lorke, and J. P. Kotthaus.

[1] For a review see, e.g., D. Weiss, in *Festkörperprobleme, Advances in Solid State Physics*, edited by U. Rössler (Vieweg, Braunschweig, 1991), Vol. 31; C. W. J. Beenakker and H. van Houten, in *Solid State Physics*, edited by H. Ehrenstein and D. Turnbull (Academic, San Diego, 1991), Vol. 44, p. 1.

[2] D. Weiss, K. v. Klitzing, K. Ploog, and G. Weimann, Europhys. Lett. **8**, 179 (1989); R. R. Gerhardts, D. Weiss, and K. v. Klitzing, Phys. Rev. Lett. **62**, 1173 (1989); R. W. Winkler, J. P. Kotthaus, and K. Ploog, Phys. Rev. Lett. **62**, 1177 (1989); K. Ismail, T. P. Smith, III, W. T. Masselink, and H. I. Smith, Appl. Phys. Lett. **55**, 2766 (1989); C. G. Smith, M. Pepper, R. Newbury, H. Ahmed, D. G. Hasko, D. C. Peacock, J. E. F. Frost, D. A. Ritchie, G. A. C. Jones, and G. Hill, J. Phys. Condens. Matter **2**, 3405 (1990); D. Weiss, K. v. Klitzing, K. Ploog, and G. Weimann, Surf. Sci. **229**, 88 (1990); H. Fang, and P. J. Stiles, Phys. Rev. B **41**, 10171 (1990); A. Lorke, J. P. Kotthaus, and K. Ploog, Phys. Rev. Lett. **64**, 2559 (1990); K. Ensslin and P. M. Petroff, Phys. Rev. B **41**, 12307 (1990); P. H. Beton, E. S. Alves, P. C. Main, L. Eaves, M. W. Dellow, M. Henini, O. H. Hughes, S. P. Beaumont, and C. D. W. Wilkinson, Phys. Rev. B **42**, 9229 (1990).

[3] A. Lorke, J. P. Kotthaus, and K. Ploog, Superlattices Microstruct. **9**, 103 (1991).

[4] K. Kern, D. Heitmann, P. Grambow, Y. H. Zhang, and K. Ploog, Phys. Rev. Lett. **66**, 1618 (1991).

[5] D. Weiss, M. L. Roukes, A. Menschig, P. Grambow, K. v. Klitzing, and G. Weimann, Phys. Rev. Lett. **66**, 2790 (1991).

[6] A. Lorke, J. P. Kotthaus, and K. Ploog, Phys. Rev. B **44**, 3447 (1991).

[7] P. G. Harper, Proc. R. Soc. London A **68**, 874 (1955); M. Ya. Azbel', Zh. Eksp. Teor. Fiz. **46**, 429 (1964) [Sov. Phys. JETP **19**, 634 (1964)]; D. R. Hofstadter, Phys. Rev. B **14**, 2239 (1976).

[8] T. Geisel, R. Ketzmerick, and G. Petschel, Phys. Rev. Lett. **66**, 1651 (1991); **67**, 3536 (1991).

[9] C. W. J. Beenakker, Phys. Rev. Lett. **62**, 2020 (1989).

[10] T. Geisel, A. Zacherl, and G. Radons, Phys. Rev. Lett. **59**, 2503 (1987); A. Zacherl, T. Geisel, J. Nierwetberg, and G. Radons, Phys. Lett. **114A**, 317 (1986).

[11] T. Geisel, J. Wagenhuber, P. Niebauer, and G. Obermair, Phys. Rev. Lett. **64**, 1581 (1990); J. Wagenhuber, T. Geisel, P. Niebauer, and G. Obermair, Phys. Rev. B **45**, 4372 (1992).

[12] See, e.g., V. I. Arnold, *Mathematical Methods of Classical Mechanics* (Springer, New York, 1989).

[13] R. Kubo, J. Phys. Soc. Jpn. **12**, 570 (1957).

[14] This condition is plausible. A rigorous but lengthy proof considering regular as well as chaotic orbits is given by R. Fleischmann, diploma thesis, Universität Frankfurt, 1991 (unpublished).

[15] We have $p_p = V_p/V$, where V_p is the volume of the outermost torus found in a Poincaré surface of section. We obtain this volume from the length of the torus and the section area, using integration theory on manifolds and considering the angle of the torus with the section plane.

[16] As the existence of orbits enclosing more than one antidot requires that the diameter of antidots is small compared to their spacing, this phenomenon could not be observed in previous far-infrared measurements [3,4].

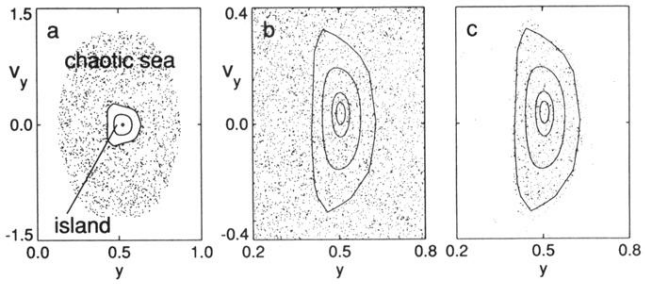

FIG. 2. (a) Poincaré surface of section [at $x(\mathrm{mod}1)=0$] for $B/B_0=1$ in the smooth potential, generated from four different initial conditions. The island of regular motion represents intersections of invariant tori for cyclotronlike orbits (radius $\approx \frac{1}{2}$) revolving around an antidot at $(x,y)=(0,0)$. (b) Randomly chosen *initial conditions* y and v_y for 5000 orbits started in a rectangular subregion covering the island and part of the chaotic sea with $x=0$ for $B/B_0=1$, and $\beta=4$. Lines indicate the intersection of invariant tori. (c) Intersection points of those orbits that in an applied electric field return to this region and thus remain "pinned."